HuR counteracts miR-330 to promote STAT3 translation during inflammation-induced muscle wasting

Souad Mubaid[a,1], Jennifer F. Ma[a,1], Amr Omer[a], Kholoud Ashour[a], Xian J. Lian[a], Brenda J. Sanchez[a], Samantha Robinson[a], Anne Cammas[b,c,d], Virginie Dormoy-Raclet[e], Sergio Di Marco[a], Sridar V. Chittur[f,g], Scott A. Tenenbaum[f,g], and Imed-Eddine Gallouzi[a,2]

[a]Department of Biochemistry, Rosalind and Morris Goodman Cancer Centre, McGill University, Montreal, QC H3G 1Y6, Canada; [b]Cancer Research Centre of Toulouse, INSERM UMR 1037, 31037 Toulouse, France; [c]Université Toulouse III Paul Sabatier, 31330 Toulouse, France; [d]Laboratoire d'Excellence "TOUCAN," 31037 Toulouse, France; [e]Laboratoire de Génétique Moléculaire, Centre Hospitalier Universitaire de Bordeaux, 33076 Bordeaux Cedex, France; [f]College of Nanoscale Sciences, State University of New York (SUNY) Polytechnic Institute, Albany, NY 12203; and [g]College of Engineering, SUNY Polytechnic Institute, Albany, NY 12203

Edited by Vishva M. Dixit, Genentech, San Francisco, CA, and approved July 18, 2019 (received for review March 26, 2019)

Debilitating cancer-induced muscle wasting, a syndrome known as cachexia, is lethal. Here we report a posttranscriptional pathway involving the RNA-binding protein HuR as a key player in the onset of this syndrome. Under these conditions, HuR switches its function from a promoter of muscle fiber formation to become an inducer of muscle loss. HuR binds to the *STAT3* (*signal transducer and activator of transcription 3*) mRNA, which encodes one of the main effectors of this condition, promoting its expression both in vitro and in vivo. While HuR does not affect the stability and the cellular movement of this transcript, HuR promotes the translation of the *STAT3* mRNA by preventing miR-330 (microRNA 330)–mediated translation inhibition. To achieve this effect, HuR directly binds to a U-rich element in the *STAT3 mRNA-3′untranslated region* (*UTR*) located within the vicinity of the miR-330 seed element. Even though the binding sites of HuR and miR-330 do not overlap, the recruitment of either one of them to the *STAT3-3′UTR* negatively impacts the binding and the function of the other factor. Therefore, together, our data establish the competitive interplay between HuR and miR-330 as a mechanism via which muscle fibers modulate, in part, STAT3 expression to determine their fate in response to promoters of muscle wasting.

HuR | STAT3 | muscle wasting | microRNA | posttranscriptional regulation

Skeletal muscle is the largest organ in the body, accounting for at least 40% of the total body mass of healthy individuals (1). The maintenance of skeletal muscle mass requires a balance between protein synthesis and protein degradation to ensure continuous renewal of muscle proteins (2, 3). Chronic diseases such as cancer, AIDS, and chronic obstructive pulmonary diseases can disrupt this balance to favor protein degradation, leading to the onset of cachexia, a syndrome characterized by rapid muscle deterioration and wasting (4). Patients who develop muscle wasting experience weakness, a lower quality of life, a decreased response to therapy, and reduced survival rates (5, 6). Despite its deleterious effects, there are currently no effective treatment options available for muscle wasting, highlighting the need to better understand the molecular mechanisms mediating this deadly syndrome, which will help identify novel targets for therapy.

It is well-accepted that one of the most common promoters of cachexia-induced muscle wasting is the excessive production of proinflammatory cytokines, such as tumor necrosis factor alpha (TNFα), IFN gamma (IFNγ), and interleukin 6 (IL-6), that is triggered by the underlying disease (5). One way by which these cytokines promote muscle loss is by activating downstream effectors in the targeted skeletal muscle, such as the transcription factors NF-κB and STAT3 (signal transducer and activator of transcription 3) (7–9). For example, IL-6 triggers the phosphorylation of STAT3 on the tyrosine 705 (Y705) residue leading to its activation, which in turn promotes the transcription of a STAT3-dependent network of procachectic genes (7, 10). On the other hand, cytokines such as IFNγ and TNFα promote muscle loss by activating the NF-κB pathway, leading to the transcription of numerous effector genes such as Atrogin1, Murf1, and iNOS (inducible nitric oxide synthase) (7, 9, 11, 12). Recent observations have uncovered that IFNγ and TNFα promote muscle loss by also activating the STAT3 pathway in a mechanism that, while independent of IL-6, involves the collaboration of STAT3 with NF-κB (7). Consistent with previous findings (13), the activation of STAT3 under these conditions is always accompanied by a significant increase in the expression levels of STAT3 protein in the targeted muscles (7). In keeping with this, increased levels in total STAT3 have been shown to enhance STAT3 activity and also correlate with poor prognosis of cancer patients (14, 15). Therefore, these observations establish that the increase in the expression levels of promoters of muscle wasting, such as STAT3, is an important molecular event behind the progression of this deadly syndrome. However, the mechanisms controlling the expression of this and other procachectic factors in muscles undergoing wasting are still poorly understood.

The control of gene expression can occur at numerous levels, including transcriptionally and posttranscriptionally. While the role of transcriptional events in the onset of muscle atrophy is well-established, the implication of posttranscriptional regulators,

Significance

Proinflammatory diseases, such as cancer, AIDS, and chronic obstructive pulmonary diseases, are often associated with a progressive loss of skeletal muscle tissue, a syndrome also known as cachexia. Cytokines trigger muscle loss by activating downstream effector pathways, including the ones driven by STAT3 protein. Although high levels of STAT3 protein are required for the onset of muscle wasting, the mechanisms modulating STAT3 expression in cachectic muscles remain elusive. Here we identify the RNA-binding protein HuR and its ability to interfere with miR-330 action as a key promoter of *STAT3* mRNA translation. Our work identifies the competition between HuR and miR-330 as a mechanism that could be targeted to design novel anticachexia therapies.

Author contributions: S.M., J.F.M., S.D.M., and I.-E.G. designed research; S.M., J.F.M., A.O., K.A., X.J.L., B.J.S., and S.R. performed research; A.C., V.D.-R., S.V.C., and S.A.T. contributed new reagents/analytic tools; S.M., J.F.M., A.O., K.A., X.J.L., S.D.M., S.A.T., and I.-E.G. analyzed data; S.M., J.F.M., and I.-E.G. wrote the paper; I.-E.G. directed the work from beginning to end; and I.-E.G. secured funding.

The authors declare no conflict of interest.

This article is a PNAS Direct Submission.

[1]S.M. and J.F.M. contributed equally to this work.

[2]To whom correspondence may be addressed. Email: imed.gallouzi@mcgill.ca.

This article contains supporting information online at www.pnas.org/lookup/suppl/doi:10.1073/pnas.1905172116/-/DCSupplemental.

such as RNA-binding proteins (RBPs) and microRNAs (miRNAs), in this process has also been reported (12, 16, 17). Several studies have associated muscle atrophy with a change in the expression levels or the functional properties of many RBPs. For example, the genetic ablation of the zinc-finger RBP Zfp106, in mice, triggers an ataxia-like syndrome that is associated with severe muscle loss, leading to the death of these animals within the first 6 mo of their birth (16). Additionally, a change in the expression levels of the ELAV family members of RBPs HuD and HuR or in their ability to interact with target mRNAs has been associated with the onset of muscle atrophy and loss triggered by underlying diseases such as spinal muscular atrophy, amyotrophic lateral sclerosis, and cancer (12, 18–20). Hence, these and other findings clearly demonstrate the importance of RBP-driven posttranscriptional events in regulating the expression of key promoters of disease-induced muscle atrophy and degeneration.

HuR and its role in both muscle fiber formation and muscle loss represent one of the best examples illustrating how an RBP could play dual and opposite functions in the same tissue (21). Indeed, HuR affects the fate of muscle fibers by modulating the stability and translation of mRNAs that either promote or hinder muscle differentiation and integrity (12, 21–25). For example, during the early steps of muscle fiber formation, a process also known as myogenesis, HuR promotes the expression of the alarmin HMGB1 by preventing miR-1192–mediated inhibition of *HMGB1* translation (24). The promyogenic function of HuR also involves the HuR-mediated stabilization of mRNA encoding key myogenic regulatory factors such as MyoD and myogenin (22, 26). In muscle fibers exposed to IFNγ and TNFα, however, HuR loses its ability to associate with the *MyoD* mRNA yet, under these conditions, HuR binds the *iNOS* mRNA to promote its expression, leading to the activation of the iNOS/NO pathway (12). Collectively, these results suggest that by switching its network of mRNA targets in response to cachectic conditions, HuR changes its function from being a promoter of muscle fiber formation to becoming a key player in the onset of muscle wasting. However, the network of procachectic mRNA targets of HuR and the way by which HuR affects their expression during muscle wasting remain elusive.

In this study, we identified *STAT3* mRNA as a HuR target during the onset of muscle wasting both in vitro and in vivo. We showed that while HuR does not affect the half-life of *STAT3* mRNA, HuR promotes *STAT3* translation by binding to a U-rich element in the 3′UTR to prevent miR-330–mediated translation inhibition. Our findings, therefore, clearly establish both HuR and miRNA-330 as key regulatory factors that modulate both STAT3 expression and STAT3-induced muscle wasting.

Results

***STAT3* Is an HuR mRNA Target in Myotubes Undergoing Wasting.** To identify the network of mRNAs that associate with HuR during muscle wasting, we used C2C12 myotubes treated with or without IFNγ/TNFα to perform RNA immunoprecipitation (RIP) coupled to cDNA microarray experiments using an anti-HuR monoclonal antibody (3A2) (12, 23, 24, 27). This in vitro cell model of muscle wasting is routinely used to mimic the effects of cytokines on muscle fibers, as seen during cachectic conditions (7, 12, 28, 29) (Fig. 1*A*). Previous observations have indicated that the expression of promoters of muscle wasting in myotubes treated with IFNγ and TNFα as well as other cytokines is usually initiated as early as 12 h posttreatment (12). Therefore, the RIP-cDNA microarray experiments mentioned above were performed on C2C12 myotubes exposed to IFNγ and TNFα for 12 h. We identified 74 mRNAs that were associated with HuR twofold or more, when compared with the messages immunoprecipitated with IgG (Dataset S1). PANTHER classification software analysis (http://www.pantherdb.org) (30) revealed that under these conditions, HuR associates with mRNA-encoding members of several signaling pathways, the most relevant of which to

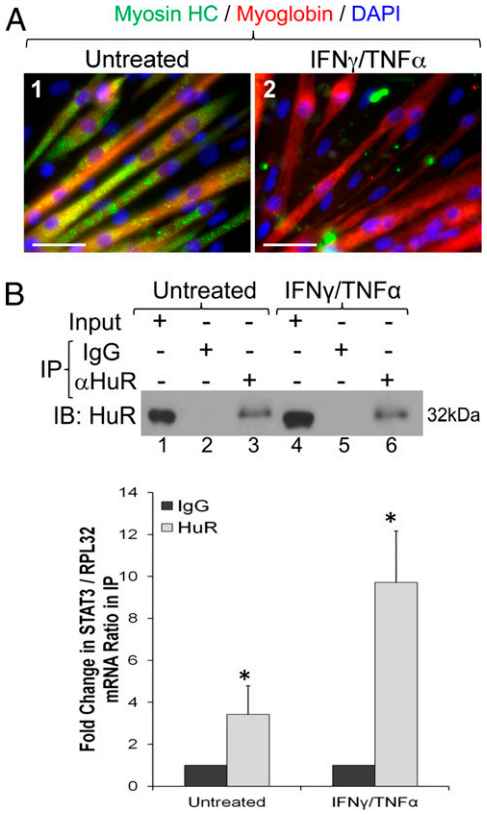

Fig. 1. HuR associates with *STAT3* mRNA in C2C12 myotubes during muscle wasting. (*A*) C2C12 myotubes were treated with or without IFNγ/TNFα for 72 h, fixed, and stained with antibodies against myosin heavy chain, myoglobin, and DAPI. Images are representative of 3 independent experiments. (Scale bars, 50 μm.) (*B*) Lysates obtained from C2C12 myotubes treated with or without IFNγ/TNFα for 24 h were used for immunoprecipitation experiments using antibodies against HuR or IgG as a negative control. Western blot experiments demonstrating immunoprecipitated HuR (*Top*) and analysis by qRT-PCR of *STAT3* mRNA associated with HuR (*Bottom*) are shown. Levels of *STAT3* in *Bottom* were standardized to *RPL32* mRNA levels. Data are representative of 3 independent experiments ($n = 3$), and error bars represent the SEM. Significant P values were calculated using the unpaired t test. *$P < 0.05$ from equivalent IgG samples. IB, immunoblotting; IP, immunoprecipitation.

cytokine-induced muscle wasting being the JAK/STAT pathway (6, 7) (*SI Appendix*, Fig. S1). A heatmap of the identified messages indicated that the *STAT3* mRNA, one of the drivers of this pathway (7), associates with HuR ∼3.5-fold more when compared with its association with the IgG control (*SI Appendix*, Fig. S2). Next, by repeating the RIP experiment followed by qRT-PCR, we validated the cDNA array data and confirmed that HuR associates with *STAT3* mRNA not only in both IFNγ/TNFα–treated C2C12 myoblasts and myotubes but also, albeit to a lesser extent, in their untreated counterparts (Fig. 1*B* and *SI Appendix*, Fig. S3). These experiments show that the *STAT3* message is a HuR mRNA target in muscle fibers undergoing wasting.

HuR Promotes STAT3 Expression during Muscle Wasting Both In Vitro and In Vivo. Previous studies have shown that, during muscle wasting, phosphorylation-mediated activation of STAT3 is concomitant with a substantial increase in its expression levels (7, 13). We confirmed these observations and showed that the increase in expression levels of STAT3 protein in myotubes exposed to IFNγ/TNFα was detected as early as 4 h posttreatment and that this effect is not associated with an increase in the levels of HuR (Fig. 2*A* and *SI Appendix*, Fig. S4). Knocking down HuR, however, significantly reduced the levels of STAT3 protein in

both untreated and treated muscle cells without affecting the steady-state levels of *STAT3* mRNA (Fig. 2 *B* and *C*). Of note, the basic level of STAT3 in untreated cells was very low compared with the treated ones, yet the absence of HuR further reduced STAT3 expression in these cells (Fig. 2*B*). We next confirmed these effects in vivo using the *Elavl1* (*HuR*) muscle-specific knockout (muHuR-KO) mice that we recently generated (31). These muHuR-KO mice appear healthy and do not differ in size when compared with their control counterparts (Fig. 2*D*). Using the Lewis lung carcinoma (LLC) model of cancer inflammation-induced muscle wasting (29, 32), we observed that the genetic ablation of HuR protected muHuR-KO mice from the LLC tumor-induced muscle loss that is normally observed in the control mice (Fig. 2 *E* and *F*). Interestingly, the protection from muscle wasting in the muHuR-KO mice correlated with a significant decrease in the expression levels of STAT3 protein when compared with its levels in control mice (Fig. 2*G*). Of note, similar to the in vitro data, depleting HuR in skeletal muscles reduced the basic expression levels in untreated muHuR-KO muscle (Fig. 2*G*). These results, therefore, demonstrate that HuR plays a key role in promoting STAT3 expression both in vitro and in vivo in muscle fibers undergoing wasting.

HuR Promotes *STAT3* Translation via a U-Rich Element in the *STAT3-3′UTR*. HuR is known to influence gene expression by modulating the stability, export, and/or translation of its target mRNAs (21,

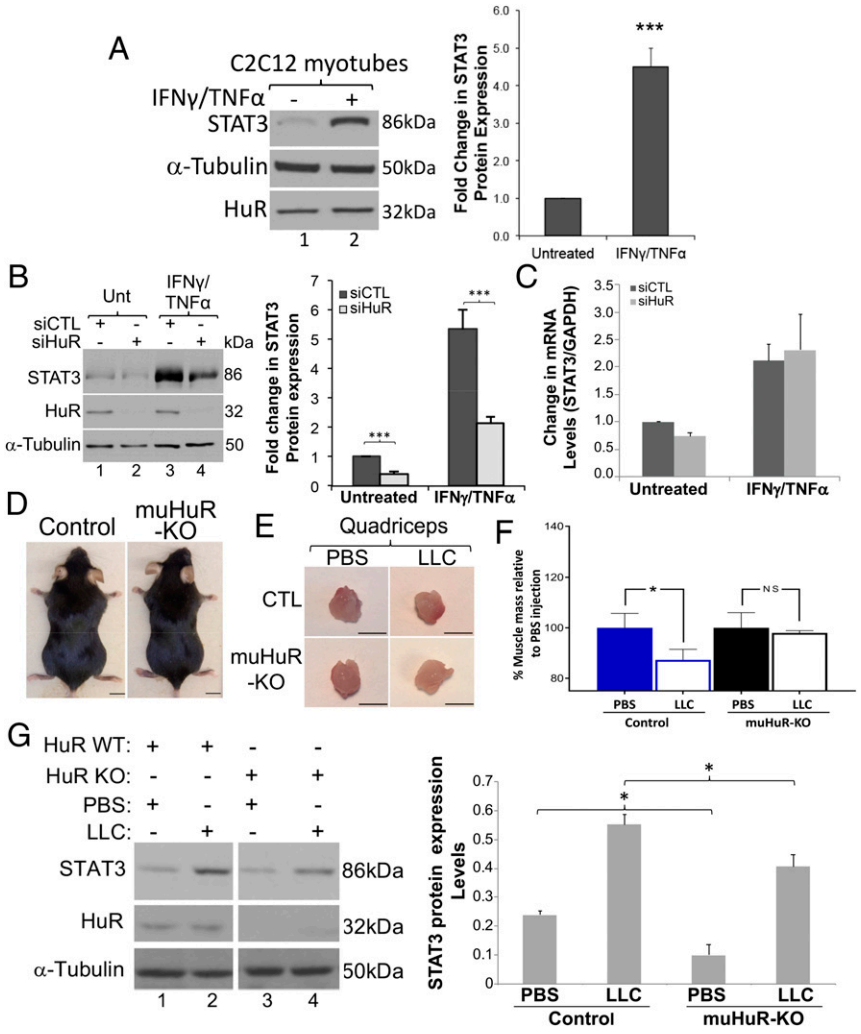

Fig. 2. HuR regulates the expression of STAT3 both in vitro and in vivo during cancer inflammation-induced muscle wasting. (*A*) Lysates obtained from C2C12 myotubes treated with or without IFNγ/TNFα for 24 h were used for Western blot analysis (*Left*) with antibodies against STAT3 and α-tubulin. (*A*, *Right*) Densitometric quantification of STAT3 signal in the Western blot relative to α-tubulin signal. (*B*) Total-cell lysates from C2C12 cells depleted or not of HuR treated with or without IFNγ/TNFα for 24 h were used for Western blot analysis (*Left*) with antibodies against STAT3, HuR, and α-tubulin. (*B*, *Right*) Densitometric quantification of STAT3 signal relative to α-tubulin signal. (*C*) Total RNA extracted from C2C12 cells treated as described in *B* was analyzed by qRT-PCR using primers specific for STAT3 and GAPDH cDNAs. Quantification of *STAT3* mRNA levels relative to GAPDH levels is shown. (*D*–*G*) Control or muHuR-KO male mice (8 to 10 wk old) were injected with PBS or LLC cells to induce muscle wasting. (*D*) Photographs of muHuR-KO and control male mice. (Scale bars, 1 cm.) (*E*) Photographs of quadriceps collected from mice described above. (Scale bars, 1 cm.) (*F*) Weight of the quadriceps described in *E*. Levels are shown as the percentage of weight remaining when compared with the PBS-treated control mice (shown as 100%). Quantifications are of 4 mice ($n = 4$). (*G*) STAT3 protein levels in quadriceps muscle obtained from mice described above were assessed by Western blot (*Left*) using antibodies against STAT3, α-tubulin (loading control), and HuR. (*G*, *Right*) Densitometric quantification of STAT3 signal relative to α-tubulin. All quantifications are of 3 independent experiments ($n = 3$) for *A*–*C* and of quadriceps muscles from 4 different mice for *G* ($n = 4$). Error bars of all quantifications represent the SEM. Significant *P* values were calculated using the unpaired *t* test. $^*P < 0.05$, $^{***}P < 0.001$ from untreated samples in *A*, siCTL untreated samples in *B*, PBS-treated control mice samples in *F*, and untreated as well as LLC-treated control mice in *G*. NS, not significant.

23, 24, 33). Our actinomycin D pulse–chase and experiments (34) and in situ hybridization experiments indicated that the depletion of HuR did not affect the half-life nor the cellular movement of the *STAT3* mRNA (*SI Appendix*, Fig. S5). We then assessed whether HuR affects the translation of the *STAT3* mRNA under muscle wasting conditions. Using sucrose-fractionation experiments, we followed the distribution of *STAT3* mRNA in polysome (P) and nonpolysome (NP) fractions in muscle cells depleted or not of HuR and treated with or without IFNγ/TNFα. Neither the knockdown of HuR nor the treatment of muscle cells with cytokines affected general translation as determined by the profile of the P and NP fractions (Fig. 3*A*). Consistent with an increase in STAT3 protein levels, as shown above (Fig. 2*A* and *SI Appendix*, Fig. S4*A*), the levels of *STAT3* mRNA recruited to polysomes dramatically increased in muscle cells treated with IFNγ/TNFα (Fig. 3*B*). The depletion of HuR in both untreated and IFNγ/TNFα–treated cells, however, prevented the recruitment of *STAT3* mRNA to polysomes (Fig. 3*B*). Together, these data clearly show that HuR promotes the translation of the *STAT3* mRNA in muscle cells exposed to wasting conditions.

It is well-established that HuR modulates the expression of its mRNA targets by directly binding to U/AU–rich elements in their 3′UTRs (21, 23, 24, 33). Hence, to delineate the mechanism by which HuR regulates STAT3 translation, we first identified the exact *cis*-element through which HuR binds to the *STAT3-3′UTR*. Sequence analysis of the *STAT3*-3′UTR revealed both U- and AU-rich elements to which HuR could potentially bind

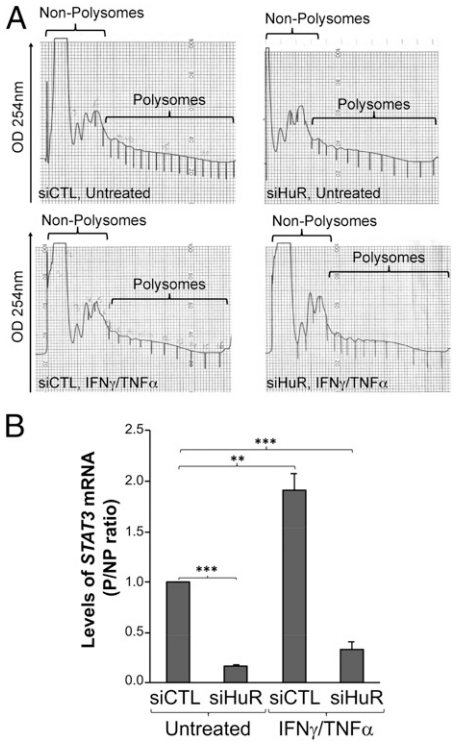

Fig. 3. HuR promotes the translation of *STAT3* mRNA. (*A*) Polysome profile of extracts obtained from C2C12 cells depleted of HuR or not and treated with or without IFNγ/TNFα for 24 h. (*B*) RNA was extracted from each fraction and qRT-PCR analysis was performed using primers for *STAT3* and *5.8S* mRNA. The levels of *STAT3* relative to 5.8S were graphed as the polysomal-to-nonpolysomal ratio. Quantifications are of 3 independent experiments ($n = 3$), and error bars represent the SEM. Significant P values were calculated using the unpaired t test. $^{**}P < 0.01$, $^{***}P < 0.001$ from untreated siCTL samples.

(*SI Appendix*, Fig. S6). To determine whether HuR directly binds to the *STAT3* mRNA through any of these elements, we performed RNA electrophoretic mobility-shift assays (REMSAs) (23, 24) using purified recombinant GST-HuR and 16 radiolabeled RNA probes that span the entire *STAT3*-3′UTR (Fig. 4*A* and *SI Appendix*, Table S1). We found that HuR forms a complex with only 5 of these RNA probes (P2, P6, P13, P14, and P16) (Fig. 4*B*). Next, the strength of HuR binding to these probes was tested by introducing RNase T1 treatment into the REMSA. In this assay, HuR–mRNA complexes are formed prior to digestion with RNase T1, which cleaves specifically after G residues (35). It is well-accepted that resistance to RNase T1 treatment will only occur as a result of a direct binding of HuR to the RNA probe (35). We observed that P2, and to a lesser extent the P16 probe, exhibited resistance to RNase T1 treatment (*SI Appendix*, Fig. S7). These data show that both P2 and P16 elements resist RNase T1 while directly bound to HuR. These data, however, do not inform on the strength/affinity, determined through calculation of the dissociation constant (K_d), of HuR binding to these sequences. Therefore, we performed REMSA (36) with increasing concentrations of GST-HuR to determine the binding affinity (K_d) of the HuR to the P2, P6, P13, P14, and P16 probes. Each one of these probes was incubated with increasing amounts of GST-HuR and the complexes were identified using REMSA as described (36) (Fig. 4 *C*, *Left*). When measuring the fraction of free probe bound to HuR, we found that HuR associated with P2 with a high affinity ($K_d \sim$ 20.5 nM). P16 as well as the other probes (P6, P13, and P14), however, did not exhibit a measurable binding affinity at the concentrations of the recombinant HuR used (Fig. 4 *C*, *Right*). Next, we determined the minimum HuR binding site within P2. To do this, we divided this probe into 4 smaller fragments, P2A, -B, -C, and -D (Fig. 4 *D*, *Top*). Based on the fact that the P2B–HuR complex generated the strongest signal in the REMSA experiment (Fig. 4 *D*, *Bottom*), we decided to further investigate the role of this *cis*-element in HuR-mediated regulation of *STAT3* translation.

To achieve this, we generated Renilla-luciferase (R-*Luc*) constructs that express wild-type *STAT3*-3′UTR (R-*Luc*-3′*STAT3*) or the *STAT3*-3′UTR from which the P2B (R-*Luc*-3′STAT3-ΔP2B) or the P16 (R-*Luc*-3′*STAT3*-ΔP16) elements were deleted (Fig. 5*A* and *SI Appendix*, Fig. S8*A*). These reporter constructs were subsequently expressed in C2C12 cells and used to determine the impact of deleting P2B or P16 on the luciferase activity. We observed that the deletion of P2B but not that of P16 significantly reduced luciferase activity (*SI Appendix*, Fig. S8*B*). Moreover, while both R-*Luc*-3′*STAT3* and R-*Luc*-3′*STAT3*-ΔP2B mRNAs were expressed to the same levels (Fig. 5*B*), the significant reduction in the luciferase activity of the R-*Luc*-3′*STAT3*-ΔP2B construct (Fig. 5*C*) correlated with the inability of its mRNA to associate with HuR (Fig. 5*D*). Therefore, these in vitro and ex vivo experiments demonstrate that HuR promotes *STAT3* mRNA translation and that this effect requires the binding of HuR to the *STAT3*-3′UTR via the U-rich P2B *cis*-element.

HuR Prevents miR-330–Mediated Translation Inhibition of *STAT3*. It is well-established that one way by which HuR modulates the translation of some of its mRNA targets is by competing or collaborating with microRNAs (24, 37). Therefore, we investigated whether this could also be the case for the HuR-mediated translation regulation of the *STAT3* mRNA. As a first step, we identified an miRNA(s) that could form a complex with HuR in C2C12 myotubes by performing a RIP experiment coupled to miRNA-sequencing analysis using antibodies against HuR or IgG as a negative control. Although 15 miRNAs were coimmunoprecipitated with HuR in C2C12 myotubes (*SI Appendix*, Table S2 and Dataset S2), only one of them, miR-330, is predicted by 3 online prediction programs (TargetScan, miRBase, and microrna.org) to target the *STAT3* mRNA. Scanning

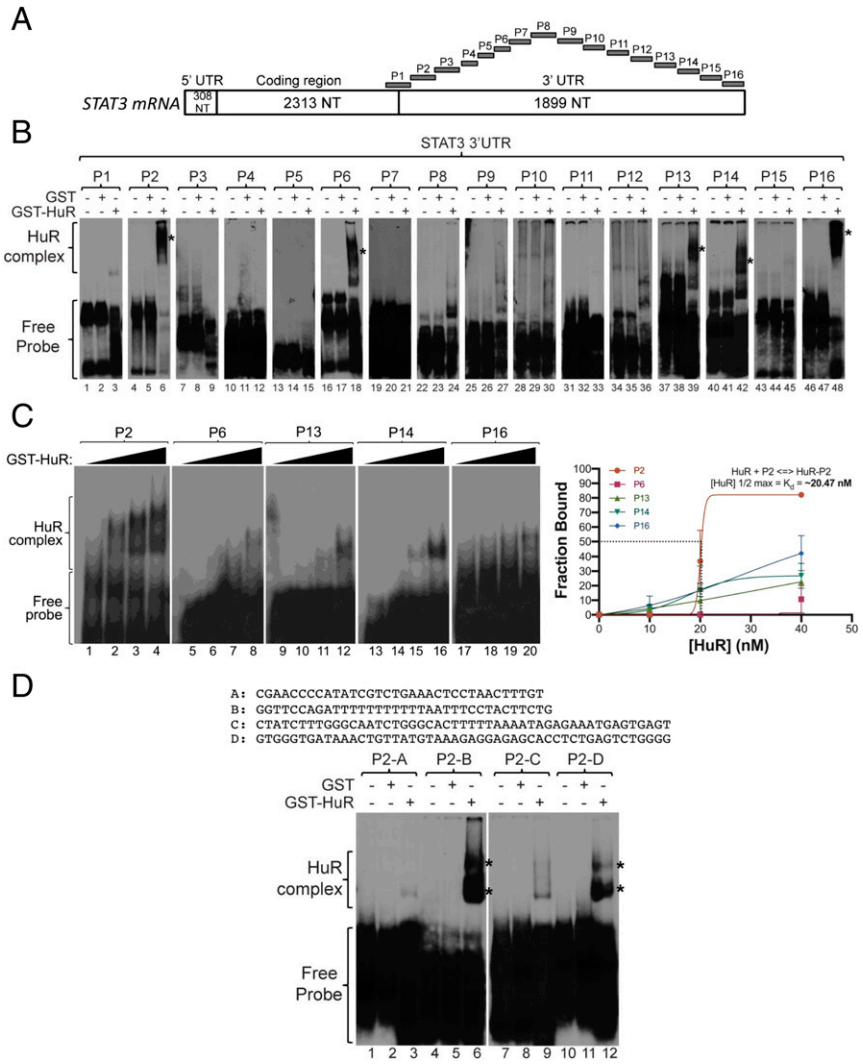

Fig. 4. HuR directly binds to a U-rich element in the 3′UTR of *STAT3* mRNA. (*A*) Schematic representation of the *STAT3* mRNA sequence. The locations of the cRNA probes covering the 3′UTR of *STAT3* mRNA used for RNA electrophoretic mobility-shift assays are indicated (P1 to P16). (*B*) Gel-shift assays were performed using recombinant GST-HuR protein or GST as a control incubated with radiolabeled cRNA probes as indicated in *A*. Representative gels of each probe from $n = 3$ experiments are shown. HuR–cRNA complex is indicated with an asterisk. (*C*, *Left*) REMSA was used to determine the dissociation constant (K_d) of HuR binding to the P2, P6, P13, P14, and P16 probes. Increasing amounts of GST-HuR protein (0, 10, 20, and 40 nM) were incubated with P2, P6, P13, P14, or P16 radiolabeled probes and complexes were resolved using REMSA as described above. (*C*, *Right*) The binding of GST-HuR with the various probes was plotted as the fraction of the associated RNA against nM GST-HuR to determine the K_d. Quantifications are of 2 independent experiments ($n = 2$), and error bars represent the SEM. (*D*) REMSAs with radiolabeled probes spanning the P2 region (P2A, P2B, P2C, and P2D) were performed to further delineate the HuR binding site. (*D*, *Top*) The nucleotide sequence of each probe used for gel shift.

the primary sequence of the *STAT3 mRNA-3′UTR* revealed that the predicted seed element of miR-330 is located 297 nt away from the HuR binding site (HuRBS) P2B (Fig. 6*A* and *SI Appendix*, Fig. S6). Although the HuRBS P2B and miR-330 binding sites could appear far apart from one another, previous observations have shown that HuR is able to interfere with miRNA-mediated translation repression even when its binding site is positioned at a considerable distance from the miRNA seed element (38). By repeating the RIP experiment followed by qRT-PCR, we validated the association of HuR with miR-330 in both untreated and IFNγ/TNFα–treated C2C12 myotubes (Fig. 6*B*) as well as in myoblasts (*SI Appendix*, Fig. S9). The observed HuR–miR-330 association is not due to an increase in the expression levels of HuR or miR-330 in response to IFNγ and TNFα (*SI Appendix*, Figs. S4*B* and S10). However, although the HuR–miR-330 complex was totally disrupted in muscle cells depleted of STAT3, the association between HuR and miR-330 was reestablished by introducing back, in these *STAT3*-knockdown muscle cells, the R-*Luc*-3′*STAT3* construct expressing an intact *STAT3*-3′UTR (Fig. 6 *C* and *D*). Together, these data clearly show that the association of HuR with miR-330 is indirect and occurs via the *STAT3*-3′UTR. It is well-established that recruiting Ago2, one of the main components of the RNA-induced silencing complex, represents one of the key steps used by miRNAs to inhibit the translation of their target mRNA (39). Interestingly, our data show that the depletion of HuR increases the association of Ago2 with both *STAT3* mRNA and miR-330 (Fig. 6 *E*–*H*), suggesting that one way by which HuR interferes with miR-330–mediated inhibition of the translation of the *STAT3* mRNA is by preventing the recruitment of Ago2.

Next, we determined the impact of the predicted seed element of miR-330, herein dubbed the miR-330 binding site (miR-330BS), on *STAT3*-3′UTR–mediated translation as well as on its association with HuR. To achieve this, we generated Renilla-luciferase

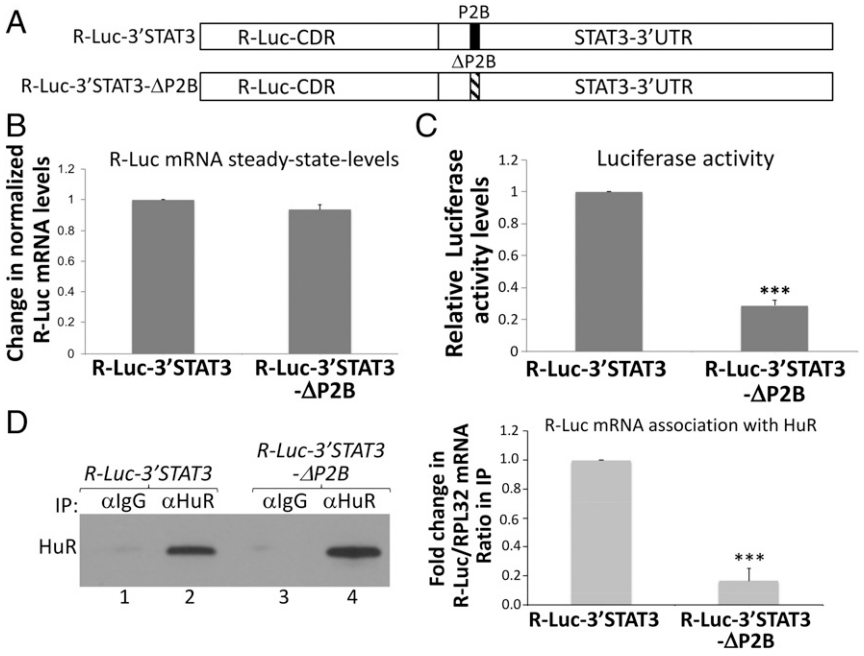

Fig. 5. P2B element is required for the *STAT3*-3′UTR–mediated translation regulation and association with HuR. (*A*) Schematic demonstrating the Renilla-luciferase (R-*Luc*) constructs (R-*Luc*-CDR, Coding Region) with the *STAT3*-3′UTR (R-*Luc*-3′*STAT3*) or the *STAT3*-3′UTR mutant in which the P2B element was deleted (R-*Luc*-3′*STAT3*-ΔP2B). (*B–D*) The reporter constructs described in A were transfected in C2C12 cells. R-*Luc* reporter mRNA steady-state levels (*B*) as well as luciferase activity (*C*) were determined for each construct. mRNA levels and luciferase activity for the R-*Luc*-3′*STAT3*-ΔP2B mRNA are shown relative to those obtained with the R-*Luc*-3′*STAT3* construct. (*D*, *Left*) Western blot showing the immunoprecipitation of HuR from cell extracts expressing R-*Luc*-3′*STAT3* or R-*Luc*-3′*STAT3*-ΔP2B mRNAs. The blot was probed with the monoclonal anti-HuR antibody. (*D*, *Right*) Total RNA from HuR immunoprecipitate was prepared and the association of R-*Luc*-3′*STAT3* or R-*Luc*-3′*STAT3*-ΔP2B mRNAs was determined by qRT-PCR. Levels were standardized to *RPL32* mRNA levels. Quantifications for *B–D* are of 3 independent experiments ($n = 3$), and error bars represent the SEM. Significant *P* values were calculated using the unpaired *t* test. ***$P < 0.001$ from R-*Luc*-3′*STAT3* samples.

constructs with the *STAT3*-3′UTR (R-*Luc*-3′*STAT3*) containing or not mutations in the miR-330BS (R-*Luc*-3′*STAT3-mut*-miR-330BS) (Fig. 7*A*). These reporter constructs were then transfected into C2C12 cells and used in luciferase expression assays as well as in immunoprecipitation experiments with the anti-HuR antibody. Although deleting the miR-330BS did not affect the steady-state levels of R-*Luc* mRNA, this mutation increased luciferase activity by threefold when compared with the activity generated by intact R-*Luc*-3′STAT3 (Fig. 7 *B* and *C*). Moreover, there was a significant increase in the association of HuR with the R-*Luc*-3′STAT3-*mut*-miR-330BS mRNA when compared with the R-*Luc*-3′STAT3 control (Fig. 7 *D* and *E*). These results clearly indicate that preventing the recruitment of miR-330 to its seed element enhances the binding of HuR to the *STAT3*-3′UTR.

The data outlined above raise the possibility that miR-330 inhibits STAT3 translation by interfering with HuR binding to the *STAT3*-3′UTR. Indeed, overexpressing an miR-330 mimic in C2C12 cells significantly decreased STAT3 expression levels and, furthermore, significantly disrupted HuR association with the *STAT3* mRNA (Fig. 8 *A* and *B*). These data suggested that HuR promotes STAT3 expression by interfering with miR-330–mediated translation inhibition. If this is true, silencing miR-330 should rescue the expression of STAT3 in muscle cells depleted of endogenous HuR. Our data indicated that the expression of an anti–miR-330 (antagomir) in C2C12 muscle cells rescued (increased by at least twofold) STAT3 protein levels in HuR-knockdown cells when compared with cells treated with small-interfering RNA (siRNA) targeting HuR (siHuR) alone (Fig. 8*C*). These results therefore indicate that HuR promotes STAT3 translation in muscle cells by binding to a *cis*-element 297 nt apart from miR-330BS, partially alleviating the translation inhibition that is normally mediated by miR-330.

Discussion

In this study, we provide evidence supporting a key role of HuR in the progression of cytokine- and cancer-induced muscle atrophy both in vitro and in vivo. We identify *STAT3* mRNA as a target of HuR and demonstrate that HuR is required for the expression of the STAT3 protein in wasting C2C12 myotubes and in skeletal muscle in mice. We also show that while HuR does not affect the stability nor the cellular movement of *STAT3* mRNA, HuR triggers muscle wasting by promoting the translation of the STAT3 protein. To achieve this, HuR binds specifically to a U-rich element in the *STAT3*-3′UTR to interfere, in part, with the miR-330–mediated inhibition of *STAT3* translation. Together, our data support a model whereby maintaining a high expression level of STAT3 protein in an HuR-dependent manner represents one of the key steps involved in the onset of muscle wasting (Fig. 8*D*).

The RIP-cDNA microarray analysis experiments clearly show that, consistent with its ability to bind a high number of target mRNAs (40, 41), HuR associates with >2,400 transcripts in untreated and fully formed myotubes (Dataset S1). As expected, many of these transcripts, such as *MyoD*, *Myogenin*, *HMGB1*, and *p21* mRNAs, are known targets of HuR and, by regulating their expression, HuR plays a key role in myogenesis (21, 22, 24, 25, 42). Surprisingly, however, in the presence of TNFα and IFNγ, HuR loses its ability to associate with the majority of its promyogenic mRNA partners and only binds to 74 messages, among which is the mRNA encoding the procachectic factor *STAT3*. These observations raise the possibility that cytokines switch the function of HuR from a promoter of muscle fiber formation to an inducer of muscle wasting. In keeping with this observation, we have previously shown that TNFα and IFNγ change the function of HuR in muscle fibers vis à vis its promyogenic mRNA

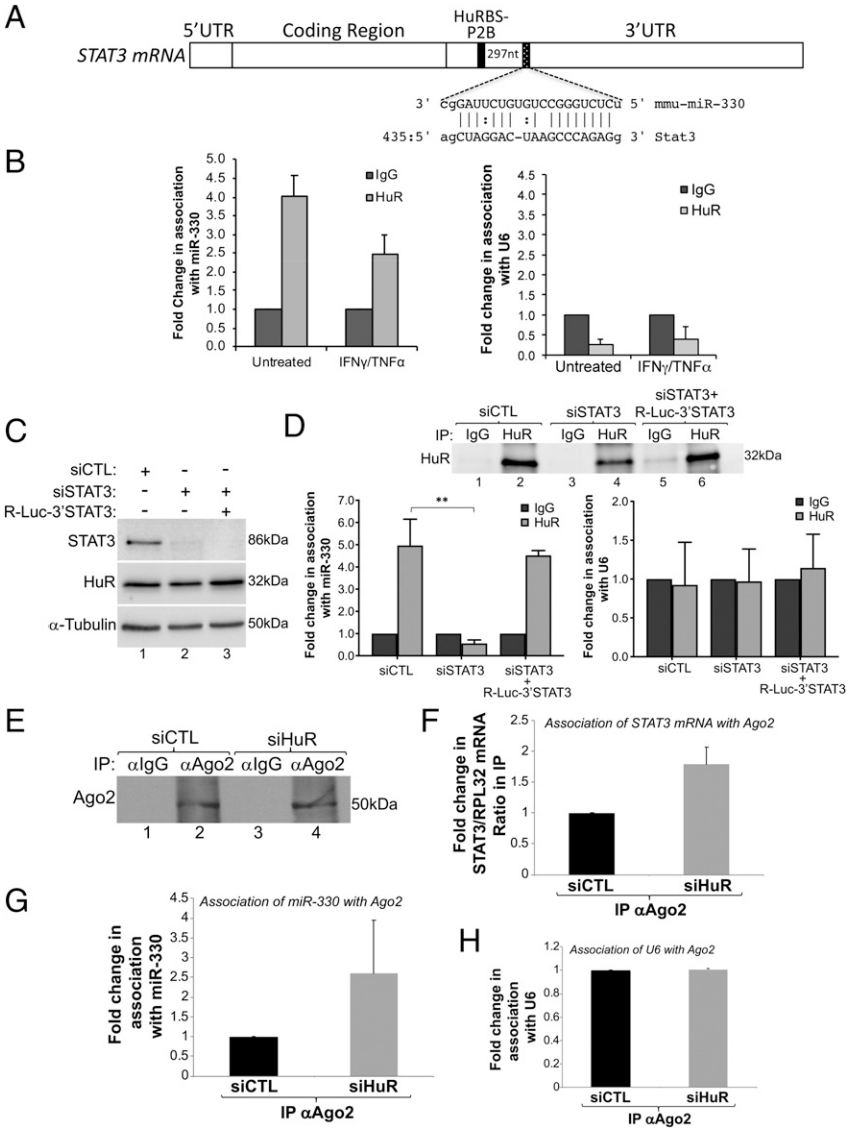

Fig. 6. HuR interacts with miR-330 in a STAT3-dependent manner. (*A*) Schematic demonstrating the alignment between the sequence of mmu-miR-330 (mmu, *Mus musculus*) and the predicted seed element in the 3′UTR of mouse *STAT3* mRNA. (*B*) Lysates obtained from C2C12 myotubes treated with or without IFNγ/TNFα for 24 h were used for immunoprecipitation experiments using antibodies against HuR or IgG as a negative control. Analysis of miRNA isolated from the immunoprecipitate was performed by qRT-PCR using primers specific for miR-330 (*Left*) or for U6 (*Right*) as a negative control. Quantifications are of 4 independent experiments ($n = 4$). (*C* and *D*) Lysates obtained from IFNγ/TNFα–treated C2C12 myoblasts expressing or not R-*Luc*-3′ STAT3 transfected with siCTL or an siRNA (siSTAT3) specifically targeting STAT3 were used for immunoprecipitation experiments using antibodies against HuR or IgG as a negative control. (*C*) Western blot analysis with antibodies against STAT3, α-tubulin, and HuR validating the knockdown of STAT3. (*D*, *Top*) Immunoprecipitated samples from C2C12 muscle cells, treated with siCTL, siSTAT3, or both siSTAT3 and expressing the R-*Luc*-3′STAT3 mRNA were used for Western blot analysis using antibodies against HuR. (*D*, *Bottom*) Analysis of miRNA isolated from the immunoprecipitate obtained using the anti-HuR antibody was performed by qRT-PCR using primers specific for miR-330 (*Left*) or for U6 (*Right*) as a negative control. Quantifications for *B–D* are of 3 independent experiments ($n = 3$), and error bars represent the SEM. Significant *P* values in *D* were calculated using the unpaired *t* test. $^{**}P < 0.01$ from siCTL samples. (*E*) Total extracts from C2C12 muscle cells expressing (siCTL) or not HuR (siHuR) were used for immunoprecipitation experiments with a rabbit monoclonal Ago2 antibody or anti-IgG antibody as a control. Ago2 immunoprecipitation was then determined by Western blot using an anti-Ago2 antibody. The Western blot shown is representative of 3 independent experiments. (*F–H*) Associated RNAs were isolated from the Ago2 immunoprecipitate, and qRT-PCR was performed using primers specific to *STAT3* and *RPL32* mRNAs (*F*), miR-330 (*G*), and U6 (*H*). The levels of *STAT3* mRNA in each IP, relative to those in the IgG IP, were normalized against the *RPL32* mRNA. Error bars represent the SEM of 2 independent experiments.

targets. Indeed, under these conditions, the HuR–*MyoD* mRNA complex is disrupted, while at the same time HuR associates with and promotes the expression of the *iNOS* mRNA (12). While these findings clearly provide strong support for a functional switch of HuR in response to extracellular assaults such as cytokines, the molecular mechanisms behind this switch are still elusive.

The fact that the depletion of HuR prevents cytokine- and cancer-induced muscle wasting both in vitro and in vivo highlights the importance of HuR protein in the progression of this deadly syndrome. Indeed, our data establish that HuR participates in this process by promoting the translation of *STAT3* mRNA, which is one of the well-established drivers of muscle loss triggered as a result of inflammatory diseases such as cancer (7, 8, 10, 43). HuR mediates this effect by directly binding to a U-rich element, P2B, in the *STAT3-3′UTR*, which consequently prevents miR-330–mediated inhibition of *STAT3* translation.

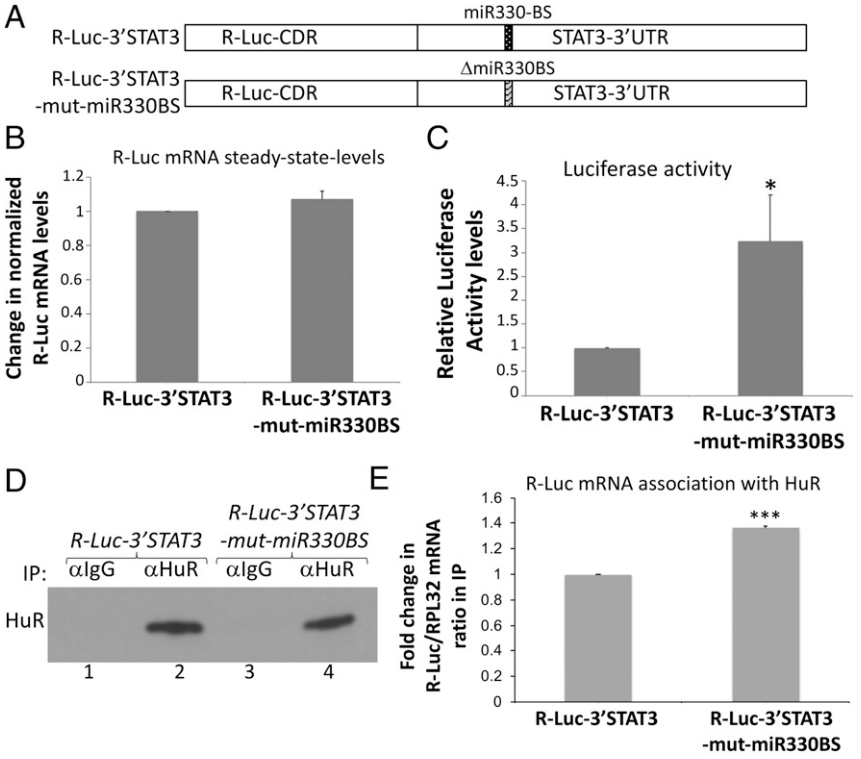

Fig. 7. miR-330 seed element regulates the expression of STAT3. (*A*) Schematic demonstrating the R-*Luc* constructs with the *STAT3*-3′UTR (R-*Luc*-3′*STAT3*) or the *STAT3*-3′UTR mutant containing a mutation of the miR-330 seed element (R-*Luc*-3′*STAT3*-mut-miR-330BS). (*B* and *C*) The reporter constructs described in *A* were transfected in C2C12 cells. R-*Luc* reporter mRNA steady-state levels (*B*) as well as luciferase activity (*C*) were determined for each construct. mRNA levels and luciferase activity for the R-*Luc*-3′*STAT3*-mut-miR-330BS mRNA are shown relative to those obtained with the R-*Luc*-3′*STAT3* construct. (*D* and *E*) Binding of HuR to the mRNA expressed from these constructs was determined by immunoprecipitating HuR (*D*) from lysates obtained from the cells described above and assessing by qRT-PCR R-*Luc* mRNA levels (*E*). Levels were standardized to *RPL32* mRNA levels. Quantifications for *B*, *C*, and *E* are of 3 independent experiments ($n = 3$), and error bars represent the SEM. Significant *P* values in *C* and *E* were calculated using the unpaired *t* test. $*P < 0.05$, $***P < 0.001$ from R-*Luc*-3′*STAT3* samples.

There are numerous examples of cross-talk between HuR and miRNA that lead to a collaborative or competitive regulation of the expression of numerous HuR mRNA targets in various systems. For example, HuR collaborates with the let-7 miRNA to inhibit the translation of *cMyc* mRNA in HeLa cells (37). In contrast, HuR, by competing with miR-195 for binding to the 3′UTR of *stromal interaction molecule 1* (*stim1*) mRNA, modulates STIM1 expression and calcium release during wound healing (44). The I.-E.G. laboratory has previously shown that HuR negates the effect of miR-1192 on HMGB1 expression despite the fact that they both simultaneously associate with the *HMGB1* mRNA in muscle cells (24). In this study, we demonstrate that the overexpression of the miR-330 mimic decreases STAT3 protein levels while the use of an antagomir targeting this miRNA rescued, in part, the decreased expression of STAT3 in cells depleted of HuR. In addition, our data also show that overexpressing the miR-330 mimic interferes with the binding of HuR with *STAT3* mRNA, suggesting a competitive interplay between these 2 *trans*-acting factors. This observation raises the question as to how both HuR and miR-330 are found within the same complex despite their competition for binding to the *STAT3* mRNA. This could be explained by the existence of a dynamic equilibrium in the binding of miR-330 and HuR to the *STAT3*-3′UTR. In fact, a dynamic equilibrium between HuR and miR-21 has been previously reported as a way to modulate the translation of *PDCD4* mRNA, where HuR directly binds to both the *PDCD4*-3′UTR as well as to the miR-21 itself (45). In our case, therefore, it is possible that the strength of the binding of HuR or miR-330 to its *cis*-element determines the outcome of STAT3 translation, promotion, or inhibition. Our data, however, clearly show that the binding of one of these *trans*-acting factors to the *STAT3*-3′UTR reduces, although not completely, the binding of the other. Although this result explains in part why these 2 *trans*-acting factors coimmunoprecipitate together in a *STAT3*-3′UTR–dependent manner, it also raises the possibility that the binding of either one of them affects the folding of the *STAT3*-3′UTR in a way that triggers the slow removal of the other factor. Testing experimentally this possibility will help determine the mechanisms behind this dynamic competitive interplay between HuR and miR-330 in modulating *STAT3* translation.

In this study, we also show that depleting miR-330 activity did not fully restore STAT3 protein levels in HuR-knockdown muscle cells, raising the possibility of the involvement of other miRNAs. Indeed, it is well-known that the *STAT3*-3′UTR is targeted by numerous miRNAs (46, 47). Therefore, it is possible that HuR also indirectly modulates the inhibition of *STAT3* translation mediated by these miRNAs. While our data showing only a partial rescue of STAT3 expression with the anti–miR-330 antagomir in HuR-depleted cells could be explained by this possibility, these results clearly link, in part, HuR effect to its ability to interfere with miR-330–mediated translation inhibition. This observation also raises the possibility that other *trans*-acting factors are involved in regulating STAT3 expression. Indeed, it has been shown that the HuR binding sites P2B and P16 that we describe in this study associate with other RBPs, such as Arid5a and CPEB1. Arid5a stabilizes *STAT3* mRNA by competing with the endoribonuclease Regnase-1 for binding to a stem-loop structure (1738–1765) that is found within the P16 element

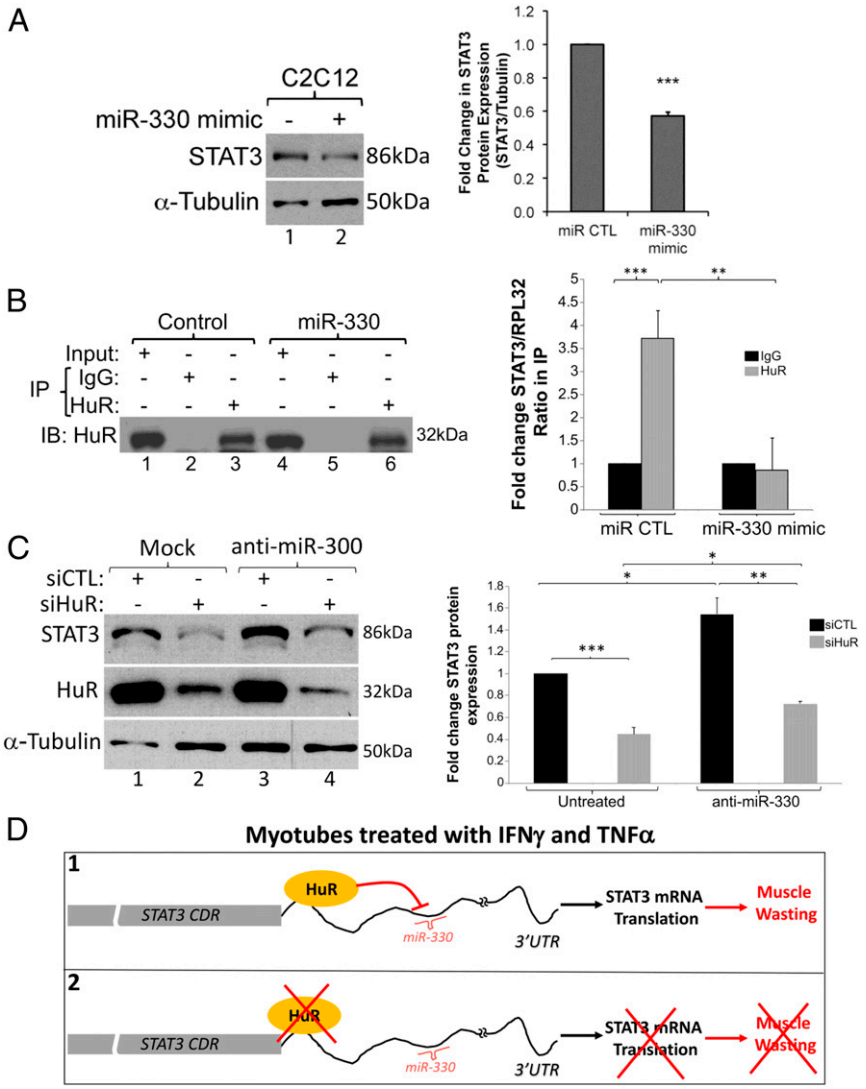

Fig. 8. HuR negates the effect of miR-330 on the expression of STAT3. (*A*) Total-cell lysate from C2C12 cells transfected with an miR-330 mimic or a control miRNA were used for Western blot analysis (*Left*) with antibodies against STAT3 and α-tubulin. (*A*, *Right*) Densitometric quantification of STAT3 signal relative to α-tubulin signal. (*B*) Lysates obtained from C2C12 myotubes transfected with miR-330 mimic or miR control (negative control) were used for immunoprecipitation experiments using antibodies against HuR or IgG as a negative control. Western blot experiments showing immunoprecipitated HuR (*Left*) and analysis by qRT-PCR of *STAT3* mRNA associated with HuR (*Right*) are shown. Levels were standardized to *RPL32* mRNA levels. (*C*) C2C12 cells were transfected with siRNA targeting HuR or a nonspecific control siRNA. The cells were then transfected with or without an antagomir against miR-330. Total-cell lysate was used for Western blot analysis (*Left*) using antibodies against STAT3, HuR, and α-tubulin. (*C*, *Right*) Densitometric quantification of STAT3 levels was normalized to α-tubulin and is shown relative to the levels observed in untreated cells transfected with the control siRNA. All quantifications are of 3 independent experiments ($n = 3$), and error bars represent the SEM. Significant *P* values were calculated using the unpaired *t* test. $^{*}P < 0.05$, $^{**}P < 0.01$, $^{***}P < 0.001$ from equivalent miR CTL (*A* and *B*) or siCTL untreated (*C*) samples. (*D*) Model depicting the HuR-dependent posttranscriptional regulation of STAT3 expression during TNFα- and IFNγ-induced muscle wasting. In myotubes exposed to TNFα and IFNγ, HuR binds to a U-rich element in the 3′UTR of STAT3 mRNA, promoting its translation. The association of HuR with its binding element prevents binding of miR-330, thus inhibiting the effect of miR-330 on the translation of the STAT3 mRNA (1). However, under these conditions, the miR-330–mediated inhibition of STAT3 expression becomes active in the absence of HuR protein (2).

(48). On the other hand, CPEB1 prevents the synthesis of STAT3 protein by binding to 2 putative U-rich elements, one of which is located within the HuR binding site P2B (49). This latter observation is consistent with our findings that the P2B but not P16 element is mainly responsible for modulating the translation of *STAT3* mRNA. However, our data do not exclude the possibility of P16 involvement in regulating STAT3 expression posttranscriptionally at other levels such as mRNA stability (48). Therefore, the possibility exists that competition or collaboration with these or other factors contributes to the HuR-mediated modulation of STAT3 expression in response to various stimuli.

Together, our data indicate that uncovering these mechanisms may lead to the identification of novel therapeutic options that can be exploited to interfere with STAT3-induced muscle wasting.

Materials and Methods

A complete description of the procedures and reagents that include plasmid construction, cell culture, miRNA prediction methods, Western blot analysis, quantitative RT-PCR, RNA immunoprecipitation, RNA electrophoretic mobility-shift assay, actinomycin D pulse–chase analysis, polysome fractionation, immunofluorescence, fluorescence in situ hybridization, muscle freezing and preparation of muscle/cell extracts, and luciferase expression/activity assays can be found in *SI Appendix, Materials and Methods*.

Animals. All experiments using animals were approved by the McGill University Faculty of Medicine, Animal Care Committee and comply with guidelines set by the Canadian Council of Animal Care. HuR muscle-specific knockout mice and their control littermates, generated on a C57BL/6 background (31), were housed in a controlled environment and provided commercial laboratory food (Harlan 2018; 18% protein rodent diet). They were grown in sterile cages with corn-cob bedding and had free access to food and water.

Lewis Lung Carcinoma Xenograft. The LLC tumors were established in 8- to 9-wk-old male muHuR-KO or control littermates as described (31). Tumors were formed due to the s.c. injections of 1×10^6 LLC cells into the right flank of the hindlimb of these mice; s.c. injections of PBS in muHuR-KO mice or control littermates were used as control. Quadriceps muscles were harvested from these mice 30 d postinjection of either PBS or LLC cells.

ACKNOWLEDGMENTS. We thank Amanda Centomare, Farah Ben Brahim, and Roman Monnet for their technical help. We also thank Derek Hall for helpful discussions and comments on the manuscript. This work is funded by a Canadian Institutes of Health Research operating grant (MOP-142399) and a Prostate Cancer Canada discovery grant (D2014-14). J.F.M. was supported by a Canadian Institutes of Health Research/Fonds de Recherche Santé Québec training grant in cancer research (FRN53888) of the McGill Integrated Cancer Research Training Program.

1. W. R. Frontera, J. Ochala, Skeletal muscle: A brief review of structure and function. *Calcif. Tissue Int.* **96**, 183–195 (2015).
2. M. Sandri, Protein breakdown in muscle wasting: Role of autophagy-lysosome and ubiquitin-proteasome. *Int. J. Biochem. Cell Biol.* **45**, 2121–2129 (2013).
3. F. Robert *et al*., Targeting protein synthesis in a Myc/mTOR-driven model of anorexia-cachexia syndrome delays its onset and prolongs survival. *Cancer Res.* **72**, 747–756 (2012).
4. M. Tsoli, G. Robertson, Cancer cachexia: Malignant inflammation, tumorkines, and metabolic mayhem. *Trends Endocrinol. Metab.* **24**, 174–183 (2013).
5. K. H. Fearon, Selective androgen receptor modulators in cancer cachexia? *Lancet Oncol.* **14**, 271–272 (2013).
6. V. E. Baracos, L. Martin, M. Korc, D. C. Guttridge, K. C. H. Fearon, Cancer-associated cachexia. *Nat. Rev. Dis. Primers* **4**, 17105 (2018).
7. J. F. Ma *et al*., STAT3 promotes IFNgamma/TNFalpha-induced muscle wasting in an NF-kappaB-dependent and IL-6-independent manner. *EMBO Mol. Med.* **9**, 622–637 (2017).
8. T. A. Zimmers, M. L. Fishel, A. Bonetto, STAT3 in the systemic inflammation of cancer cachexia. *Semin. Cell Dev. Biol.* **54**, 28–41 (2016).
9. D. T. Hall, J. F. Ma, S. D. Marco, I. E. Gallouzi, Inducible nitric oxide synthase (iNOS) in muscle wasting syndrome, sarcopenia, and cachexia. *Aging (Albany N.Y.)* **3**, 702–715 (2011).
10. A. Bonetto *et al*., JAK/STAT3 pathway inhibition blocks skeletal muscle wasting downstream of IL-6 and in experimental cancer cachexia. *Am. J. Physiol. Endocrinol. Metab.* **303**, E410–E421 (2012).
11. D. Cai *et al*., IKKbeta/NF-kappaB activation causes severe muscle wasting in mice. *Cell* **119**, 285–298 (2004).
12. S. Di Marco *et al*., NF-kappa B-mediated MyoD decay during muscle wasting requires nitric oxide synthase mRNA stabilization, HuR protein, and nitric oxide release. *Mol. Cell. Biol.* **25**, 6533–6545 (2005).
13. L. Zhang *et al*., Stat3 activation links a C/EBPδ to myostatin pathway to stimulate loss of muscle mass. *Cell Metab.* **18**, 368–379 (2013).
14. P. Wu *et al*., Prognostic role of STAT3 in solid tumors: A systematic review and meta-analysis. *Oncotarget* **7**, 19863–19883 (2016).
15. Y. H. Xu, S. Lu, A meta-analysis of STAT3 and phospho-STAT3 expression and survival of patients with non-small-cell lung cancer. *Eur. J. Surg. Oncol.* **40**, 311–317 (2014).
16. D. M. Anderson *et al*., Severe muscle wasting and denervation in mice lacking the RNA-binding protein ZFP106. *Proc. Natl. Acad. Sci. U.S.A.* **113**, E4494–E4503 (2016).
17. J. Li *et al*., miR-29b contributes to multiple types of muscle atrophy. *Nat. Commun.* **8**, 15201 (2017).
18. F. Farooq, S. Balabanian, X. Liu, M. Holcik, A. MacKenzie, p38 mitogen-activated protein kinase stabilizes SMN mRNA through RNA binding protein HuR. *Hum. Mol. Genet.* **18**, 4035–4045 (2009).
19. C. Fallini, G. J. Bassell, W. Rossoll, The ALS disease protein TDP-43 is actively transported in motor neuron axons and regulates axon outgrowth. *Hum. Mol. Genet.* **21**, 3703–3718 (2012).
20. P. Milani *et al*., Posttranscriptional regulation of SOD1 gene expression under oxidative stress: Potential role of ELAV proteins in sporadic ALS. *Neurobiol. Dis.* **60**, 51–60 (2013).
21. C. von Roretz, P. Beauchamp, S. Di Marco, I. E. Gallouzi, HuR and myogenesis: Being in the right place at the right time. *Biochim. Biophys. Acta* **1813**, 1663–1667 (2011).
22. P. Beauchamp *et al*., The cleavage of HuR interferes with its transportin-2-mediated nuclear import and promotes muscle fiber formation. *Cell Death Differ.* **17**, 1588–1599 (2010).
23. A. Cammas *et al*., Destabilization of nucleophosmin mRNA by the HuR/KSRP complex is required for muscle fibre formation. *Nat. Commun.* **5**, 4190 (2014).
24. V. Dormoy-Raclet *et al*., HuR and miR-1192 regulate myogenesis by modulating the translation of HMGB1 mRNA. *Nat. Commun.* **4**, 2388 (2013).
25. K. van der Giessen, S. Di-Marco, E. Clair, I. E. Gallouzi, RNAi-mediated HuR depletion leads to the inhibition of muscle cell differentiation. *J. Biol. Chem.* **278**, 47119–47128 (2003).
26. A. Figueroa *et al*., Role of HuR in skeletal myogenesis through coordinate regulation of muscle differentiation genes. *Mol. Cell. Biol.* **23**, 4991–5004 (2003).
27. S. A. Tenenbaum, C. C. Carson, P. J. Lager, J. D. Keene, Identifying mRNA subsets in messenger ribonucleoprotein complexes by using cDNA arrays. *Proc. Natl. Acad. Sci. U.S.A.* **97**, 14085–14090 (2000).
28. S. Di Marco *et al*., The translation inhibitor pateamine A prevents cachexia-induced muscle wasting in mice. *Nat. Commun.* **3**, 896 (2012).
29. D. T. Hall *et al*., The AMPK agonist 5-aminoimidazole-4-carboxamide ribonucleotide (AICAR), but not metformin, prevents inflammation-associated cachectic muscle wasting. *EMBO Mol. Med.* **10**, e8307 (2018).
30. H. Mi *et al*., PANTHER version 11: Expanded annotation data from gene ontology and reactome pathways, and data analysis tool enhancements. *Nucleic Acids Res.* **45** (D1), D183–D189 (2017).
31. J. B. Sánchez *et al*., Depletion of HuR in murine skeletal muscle enhances exercise endurance and prevents cancer-induced muscle atrophy. *Nat. Commun.* (Forthcoming 2019).
32. M. D. Deboer, Animal models of anorexia and cachexia. *Expert Opin. Drug Discov.* **4**, 1145–1155 (2009).
33. K. Abdelmohsen, Y. Kuwano, H. H. Kim, M. Gorospe, Posttranscriptional gene regulation by RNA-binding proteins during oxidative stress: Implications for cellular senescence. *Biol. Chem.* **389**, 243–255 (2008).
34. G. L. Drury, S. Di Marco, V. Dormoy-Raclet, J. Desbarats, I. E. Gallouzi, FasL expression in activated T lymphocytes involves HuR-mediated stabilization. *J. Biol. Chem.* **285**, 31130–31138 (2010).
35. S. Di Marco, Z. Hel, C. Lachance, H. Furneaux, D. Radzioch, Polymorphism in the 3′-untranslated region of TNFalpha mRNA impairs binding of the post-transcriptional regulatory protein HuR to TNFalpha mRNA. *Nucleic Acids Res.* **29**, 863–871 (2001).
36. L. Zhang, J. E. Lee, J. Wilusz, C. J. Wilusz, The RNA-binding protein CUGBP1 regulates stability of tumor necrosis factor mRNA in muscle cells: Implications for myotonic dystrophy. *J. Biol. Chem.* **283**, 22457–22463 (2008).
37. H. H. Kim *et al*., HuR recruits let-7/RISC to repress c-Myc expression. *Genes Dev.* **23**, 1743–1748 (2009).
38. P. Kundu, M. R. Fabian, N. Sonenberg, S. N. Bhattacharyya, W. Filipowicz, HuR protein attenuates miRNA-mediated repression by promoting miRISC dissociation from the target RNA. *Nucleic Acids Res.* **40**, 5088–5100 (2012).
39. M. R. Fabian, N. Sonenberg, W. Filipowicz, Regulation of mRNA translation and stability by microRNAs. *Annu. Rev. Biochem.* **79**, 351–379 (2010).
40. C. O. Nicholson, M. Friedersdorf, J. D. Keene, Quantifying RNA binding sites transcriptome-wide using DO-RIP-seq. *RNA* **23**, 32–46 (2017).
41. L. E. Simone, J. D. Keene, Mechanisms coordinating ELAV/Hu mRNA regulons. *Curr. Opin. Genet. Dev.* **23**, 35–43 (2013).
42. K. van der Giessen, I. E. Gallouzi, Involvement of transportin 2-mediated HuR import in muscle cell differentiation. *Mol. Biol. Cell* **18**, 2619–2629 (2007).
43. A. Bonetto *et al*., STAT3 activation in skeletal muscle links muscle wasting and the acute phase response in cancer cachexia. *PLoS One* **6**, e22538 (2011).
44. R. Zhuang *et al*., miR-195 competes with HuR to modulate stim1 mRNA stability and regulate cell migration. *Nucleic Acids Res.* **41**, 7905–7919 (2013).
45. D. K. Poria, A. Guha, I. Nandi, P. S. Ray, RNA-binding protein HuR sequesters microRNA-21 to prevent translation repression of proinflammatory tumor suppressor gene programmed cell death 4. *Oncogene* **35**, 1703–1715 (2016).
46. A. Haghikia, M. Hoch, B. Stapel, D. Hilfiker-Kleiner, STAT3 regulation of and by microRNAs in development and disease. *JAKSTAT* **1**, 143–150 (2012).
47. M. Kurdi, C. Zgheib, G. W. Booz, Recent developments on the crosstalk between STAT3 and inflammation in heart function and disease. *Front. Immunol.* **9**, 3029 (2018).
48. K. Masuda *et al*., Arid5a regulates naive CD4+ T cell fate through selective stabilization of Stat3 mRNA. *J. Exp. Med.* **213**, 605–619 (2016).
49. I. M. Alexandrov *et al*., Cytoplasmic polyadenylation element binding protein deficiency stimulates PTEN and Stat3 mRNA translation and induces hepatic insulin resistance. *PLoS Genet.* **8**, e1002457 (2012).